T.Z. WOŹNIAK[*], Z. RANACHOWSKI[**], P. RANACHOWSKI[**], W. OZGOWICZ[***], A. TRAFARSKI[*]

THE APPLICATION OF NEURAL NETWORKS FOR STUDYING PHASE TRANSFORMATION BY THE METHOD OF ACOUSTIC EMISSION IN BEARING STEEL

ZASTOSOWANIE SIECI NEURONOWYCH DO BADANIA PRZEMIAN FAZOWYCH W STALI ŁOŻYSKOWEJ METODĄ EMISJI AKUSTYCZNEJ

The research was carried out on steel l00CrMnSi6-4 under isothermal austempering resulting in forming the duplex structure: martensitic and bainitic. The kinetics of transformation was controlled by the acoustic emission method. Complex phase transformations caused by segregation and carbide banding occur at the low-temperature heat treatment of bearing steel. At the temperature close to M_S, a certain temperature range occurs where an effect of the first product of prior athermal martensite on the bainitic transformation can be observed. In the registered signal about 15 million various events were registered. There were considered three types of acoustic emission events (of high, medium and low energy), with relatively wide sections and with different spectral characteristics. It was found that the method of acoustic emission complemented by the application of neural networks is a sensitive tool to identify the kinetics of bainitic transformation and to show the interaction between martensitic and bainitic transformations.

Keywords: Bearing steel, austempering, lower bainite, acoustic emission, neural networks

Badania realizowano na stali l00CrMnSi6-4 poddanej hartowaniu izotermicznemu, prowadzącemu do utworzenia struktury duplex: martenzytyczno-bainitycznej. Kinetykę przemian kontrolowano metodą emisji akustycznej. Przy niskotemperaturowej obróbce cieplnej stali łożyskowej występują złożone przemiany fazowe spowodowane segregacją i pasmowością węglików. W temperaturze zbliżonej do M_S, występuje pewien zakres temperatury, gdzie zaznacza się oddziaływanie wcześniejszego produktu przemiany martenzytycznej na przemianę bainityczną. W zarejestrowanym sygnale zarejestrowano około 15 milionów różnych zdarzeń. Uwzględniono trzy rodzaje zdarzeń emisji akustycznej (o wysokiej, średniej i niskiej energii) o względnie szerokich przedziałach, o różnej charakterystyce widmowej. Stwierdzono, że metoda emisji akustycznej uzupełniona o zastosowanie sieci neuronowych jest czułym narzędziem do identyfikacji kinetyki przemiany bainitycznej oraz oddziaływania przemiany martenzytycznej na przemianę bainityczną.

1. Introduction

The concept of forming microstructures with residual austenite called Quenching and Partitioning – Q&P) [1] has been considering recently in the context of heat treatment. This process requires both cooling austenite below the temperature when the martensitic transformation starts and enriching the unchanged austenite into carbon. Then the austenite is transformed into lower-bainite, similarly to the "swing back" effect [2-8]. The phenomenon shows clear rapid austenite decomposition near M_S temperature. Isothermal quenching/austempering near M_S induces a phenomenon in which the preceding product of martensite transformation affects bainitic transformation [8, 9]. A number of researches prove that bainite nucleation takes place on the prior athermal martensite (PAM) so called *midribs* in the range of the accelerated transformation start [6, 8, 10].

In the recent years, high-resistant martensitic and bainitic steels with a considerate participation of residual austenite have been worked out, finding their application in automotive, defensive and air industries [11]. Isothermal austempering is also widely used in antifriction bearing industry. The combination of martensite and bainite structures in particular improved mechanical properties [12]. A new way of heat treatment in steel 100CrMnSi6-4 is gradual austempering [13]. Such a heat treatment consists in forming martensite with endurance below temperature M_S followed by a typical bainitic transformation. The objective of the research is to identify phase transformations after isothermal austempering in bearing steels with using neural networks, including the results of microscopy, dilatometry and acoustic emission (AE). The present study also shows how the structure heterogeneity caused by primary carbide banding in steel 100CrMnSi6 affects the kinetics of phase transformations that determine the occurrence

[*]   KAZIMIERZ WIELKI UNIVERSITY, INSTITUTE OF TECHNOLOGY, 30 CHODKIEWICZA STR., 85-064 BYDGOSZCZ, POLAND

[**] POLISH ACADEMY OF SCIENCES, INSTITUTE OF FUNDAMENTAL TECHNOLOGICAL RESEARCH, 5B PAWIŃSKIEGO STR., 02-103 WARSZAWA, POLAND

[***] SILESIAN UNIVERSITY OF TECHNOLOGY, INSTITUTE OF ENGINEERING AND BIO-MATERIALS, 18A KONARSKIEGO STR., 44-100 GLIWICE, POLAND

of acoustic emission effects. AE in combination with neuron networks applied in this study is a new and promising research technique [14].

2. Experimental procedure

Steel 100CrMnSi6-4 (EN ISO 683-17:1999) was used for the research, Table 1.

Chemical composition of steel (wt %)

C	Mn	Cr	Si	S	P
0.95	1.10	1.47	0.57	0.007	0.014

The samples were austenitized at 950°C for 0.5 hour and immersed in hot oil of constant temperature 160°C). In order to define temperature M_S for the steel 100CrMnSi6-4, dilatometric research was conducted with use of the Adamel Lhomargy 04 dilatometer, for six samples l=12 mm long and Φ=2 mm in diameter.
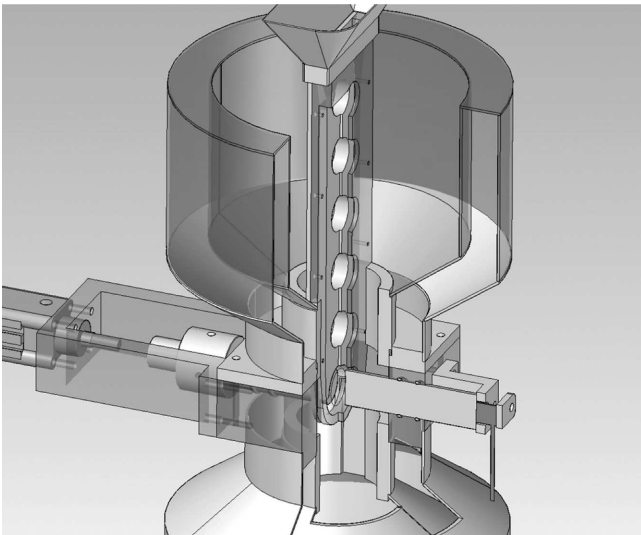

Fig. 1. View of the stand in the Solid Edge program for the acoustic emission testing at austempering

The research by the AE method was carried out in a special device, Fig. 1. The particular elements of the research and measurement equipment are a new solution, constructed for generating and registering AE signals during isothermal austempering. The process of AE signal study was running in the following way: 1) preparing samples g=2 ±0.01 mm thick and Φ=45 mm in diameter, 2) warming samples for app. 30 min. in a furnace at 950°C, 3) taking them out fast and moving the samples to the guide immersed in warmed oil to 4) record acoustic signals in the program and their further processing.

Full information on microstructure was obtained after etching the microsection surface with use of a popular reagent nital and with Villel's reagent [15]. Microscopic research was made by using a metallographic reversed light microscope of EPIPHOT 200 type produced by NIKON, equipped with a colour digital camera CCD of 2 Mpixel resolution.
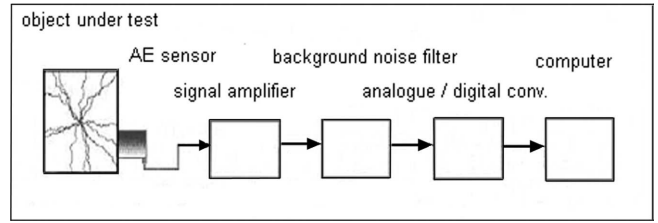

Fig. 2. Block diagram of the stand for testing acoustic emission, broad-band sensor of WD type (20 kHz–900 kHz), card ADLINK 9812 with frequency 1,200 kHz, data format bipolar mode 5V, RMS value of the noise at the input of the preamplifier was app. 12-15 microvolts, after amplifying 2.000 times (66 dB) 24 mV

The signals were registered by AE Signal Analyser, Fig. 2 with sampling 1.2 MHz. The system resolution is 0.8 μs. However, considering the applied algorithm of the event detection, the event time precision equals to three signal samples, i.e 2.4 μs. The algorithm analysed digital signal samples in scale 0-2048 (for physical range 0-5V).
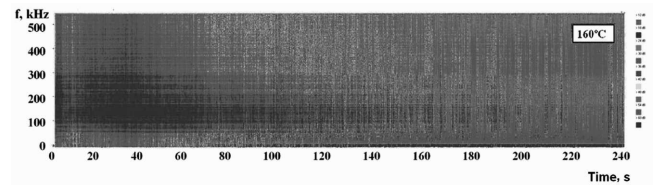

Fig. 3. View of an exemplary image generated by program presenting acoustogram

A window algorithm STFT (Short Time Fourier Transform) with a Hamming window was used to draw a spectrogram, Fig. 3. Each frame was received from 17640 signal samples. The spectrum was calculated from the next 1647 samples inside the frame, where the signal showed the maximum value. The procedure of determining a spectral density function $A(\omega)$ makes it possible to compare the power of the measured signal for selected frequency ranges, i.e. to determine the spectrum of the AE signal power. A large number of AE events from various phase transformations are registered during measurements.
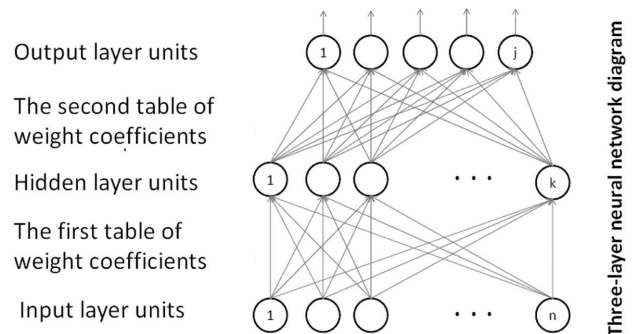

Fig. 4. Neural network learning of acoustic emission neural signals

The signal-classifying procedure uses the values of the neural network, Fig. 4. The software using neural networks consists of three programs. They help to follow the activity changes for AE events generated from various processes. The events differ as regards spectral characteristics and energy. The research identified three groups of AE events in the tested

signal: high-energy events – over 10.000 pJ, average energy events – from 1.000 to 10.000 pJ, low energy events – below 1.000 pJ. Kinetic curves for bainite and lower bainite accelerated by small amounts of PAM were obtained by filtering the generated AE signal with use of the neural network. The first program for neural networks divides the registered signal formatted wav into segments with time period 7.35 ms. In each segment, AE events are recorded and the average energy of the events is determined. 80 samples of the signal neighbouring on the signal maximum were used to determine the spectral density function. Using the next program, it is possible to prepare a neural network for learning procedure. Spectral characteristics in neural classification are transformed into relevant sets of zeros and ones. The sets are vectors of characteristics connected with the classes of AE signals. The information found in the vectors of characteristics is transmitted to weight coefficient tables, which are structures making a part of neural network. The structure is composed of units called neurons which, in turn, are arranged into two groups called layers. Each of the neurons from the preceding layer has a contact with the neurons from the next layer. The first table of weight coefficients contains 10.000 coefficients imitating links between the units of the input layer and the 50 units of the next layer. The other table includes 300 coefficients imitating links between the units of the second layer and the six units of the input layer. The signal is generated on six inputs of the network, depending on the vector form of the characteristics given for the network input. In order to store in vector weight tables the characteristics of standards used for classification of AE signals, an algorithm respecting inter-neural connection weight changes was applied, known as "reverse propagation of error". Each neuron from the preceding layer has a contact with the neurons from the next layer. If the input signal from the neural network exceeds the threshold value, i.e. the value 0.9, the result file of the procedure registers the found-signal event, with spectral characteristics close to the defined pattern.

3. Results of the research

3.1. Microstructure Analysis and dilatometry results

Bainitic transformation at 160°C (Fig. 5) occurs in two overlapping stages. In the first stage takes place the nucleation of the small amounts of prior athermal martensite during cooling and the further growth of accelerated bainite. The next stage shows the nucleation and growth of typical lower bainite.

The metallographic research for steel 100CrMnSi6-4 revealed microstructure banding, Fig. 6 a). The banding is defined as bright bands of almost pure martensitic structure, poor in carbides. When the austenitizing temperature increases, the danger of grain growth and hardening deformation also rises in these areas. Bright martensitic bands occur next to the dark ones with martensitic and bainitic matrix and with higher content of carbides, Fig. 6 b). For bearing steel bands with higher content of carbides, the solid solution is richer in carbon, chromium and manganese after austenitizing than in neighbouring bands. However, for stable austenitizing temperature, the increase in total carbon content corresponds with a decrease in chromium balance content in austenite. Apart from

various microhardness of the bands, the structure is characterised by various sizes of plates of lower bainite, the size of which depends on the size of austenite grains.
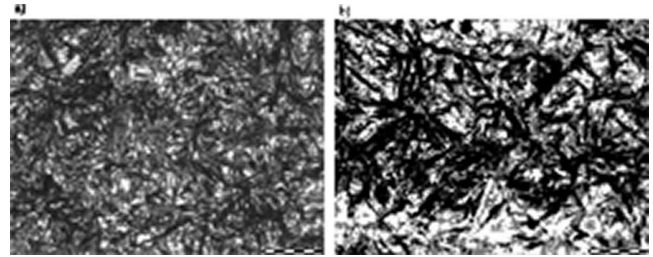

Fig. 5. Image of microstructure after austempering with isothermal transformation at 160°C a) during 8400s etched lower bainite accelerated by small amounts of prior athermal martensite (4% nital etching), b) during 240 s, the image after digital processing with visible plates of lower bainite accelerated by small amounts of prior athermal martensite in black colour, bainite in grey and residual austenite in white
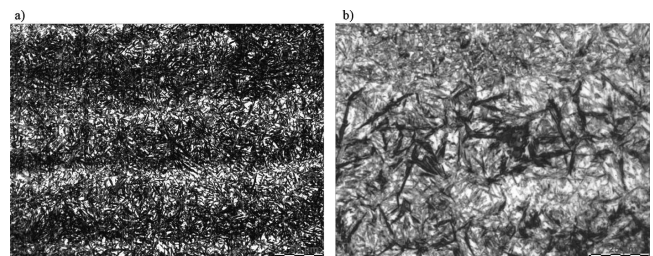

Fig. 6. Microstructure heterogeneity for steel 100CrMnSi6-4 caused by carbide banding along rolling after isothermal austempering at 160°C during 540s a) secondary banding as a result of matrix austempering diversity, b) enlarged fragment of the microstructure image within martensitic and bainitic matrix (etching by nital), banding size 7.3 by Stahl-Eisen-Prüfblatt SEP 1520 (4% nital etching)

The applied values of the isothermal austempering temperature cause the diffusion of carbon to the areas of untransformed austenite (partitioning), which is connected with forming accelerated lower bainite by small amounts of PAM visible on microscopic images and then with forming lower bainite, Fig. 7.
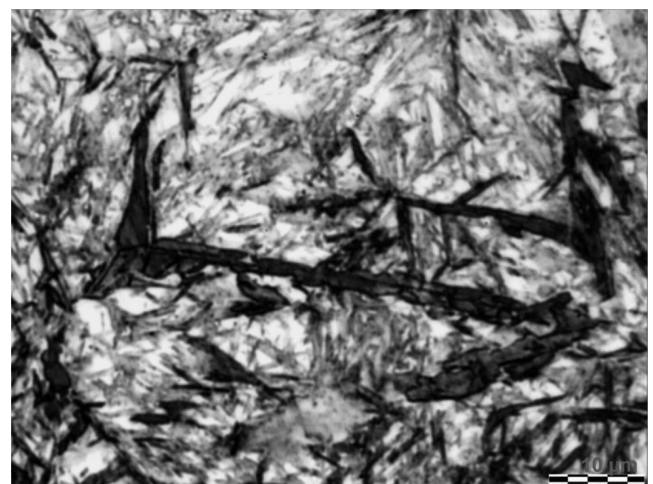

Fig. 7. Observation of microstructure details with visible lower bainite accelerated by small amounts of prior athermal martensite after austempering with isothermal transformation at 160°C during 3 min., etching with nital

As it has been observed on dilatometric curves in Fig. 8 a), martensitic transformation occurs in a defined temperature range. The division into different ranges is made by gradients of alloy element concentration in austenite caused by dissolving carbides during austenitizing. The point marked as M_{SI}, defined as linearity deviation on a dilatometric curve, corresponds to the point where a thermal decrease of the austenite volume swings aside from linearity as a result of small amounts of PAM formation in areas with locally poor carbon content and carbide-forming elements. Very poor intensity of transformations is probably caused by martensitc transformation of the areas with relatively small volume fraction. This type of linearity deviation can result from releasing carbides during the cooling as well [16]. However, the maximal number of AE events has also been observed near M_{SI}=157°C, which suggests small amounts of PAM formation. A slightly higher effect of dilatometric changes was found at M_{SII} =119°C, which suggests a partial martensitic transformation in the areas where austenite shows lower alloy element concentration than in other areas. As marked in Fig. 8 b) presenting a fragment of a dilatometric curve, the basic mass martensitic transformation starts at minimum M_{SIII}=110°C. As it results from calculations based on interrelations made by Bohemen and Sietsma [17], the temperature M_S is 153°C. For temperature 160°C, at which the research was carried out, near M_S, a lot of plates of lower bainite accelerated by small amounts of PAM are observed.
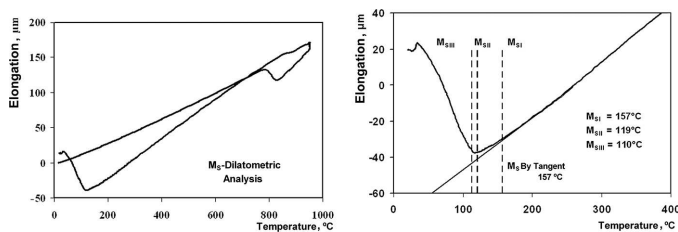

Fig. 8. Dilatometry results: a) example of dilatometric curves, b) fragment of the curve from fig. a) during cooling, with marked characteristic points

3.2. Results of acoustic emission signals

The AE system may take samples at 1.2 MHz. This sampling rate is sufficient to measure signals at frequencies up to 0.6 MHz. In order to visualize individual signals, which are AE at different temperatures of austempering, they were fragmented, as shown graphically in Fig. 9. At 160°C signal rate is very high at the start of quenching. With the applied resolution the individual bursts overlap and create an image of a continuous character. Such a division of AE signals is purely arbitrary, because in this continuous image of signal the individual events can also be distinguished [18-20].

In the austempering temperature of 160°C a high power of AE signals occurs. Because of technical limitations of longer digital recording, the signal recording was additionally continued after further 20 minutes of break. The results of tests shown in Fig. 10 confirm that the time of AE occurrence may be much longer than 4 minutes in certain circumstances. (The second stage of recording AE events is indicated by an arrow). The results of signal energies are very high both at

I stage of recording time and at II stage of recording time. The energy of signals at II stage at 160°C is still so high that it is comparable to the energy of signals and I stage (240 s). During first 4 minutes, the frequency of the occurrence of AE events is so high that the curve representing energy changes often runs continuously. The incidence of events gradually decreases with the increase in transformation time.
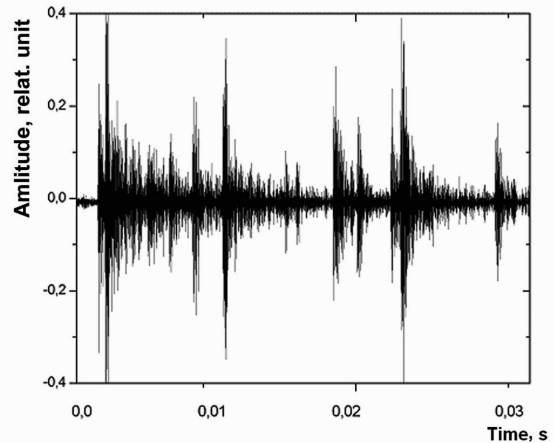

Fig. 9. Fragments of signal images in 40ms wide periods at isothermal transformation temperature 160°C in time period between 30th and 32th second
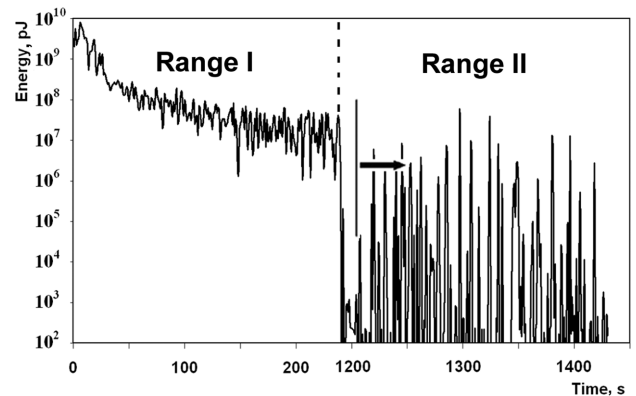

Fig. 10. Power of acoustic emission signals in time of first 4 minutes from the start (I stage of recording) and through further 4 minutes, after 20 minutes of time break marked with arrow (II stage of recording). Isothermal quenching at 160°C

In order to detect AE signals and spectrum components, a threshold level of AE signal was adopted, slightly more than background noise. If the AE signal exceeded the threshold both in positive and negative directions, the event were recorded. For calculations of the number of events, an exceedance of the threshold of 1.000 and the same level of drops were taken into account. The results of these calculations were adapted to five-voltage scale. In order not to include noise interferences as an event, in the calculation procedure, the sum of the two previous samples was subtracted from the sum of the two adjacent samples. If this difference exceeded 1.000 units, a start of the event was signalized and time was measured up to the moment that another difference was less than 1.000 units. Because of the algorithm applied, the shortest event included three samples of AE signal, i.e. 2.4 microseconds. The results of calculations signal powers (the sum of energy at the time

of any subsequent seconds) is shown in Fig. 10. The energy of AE signals was determined using the formula for triangle area calculated as a half of the product of square of the voltage V_{max} and the time of AE event.
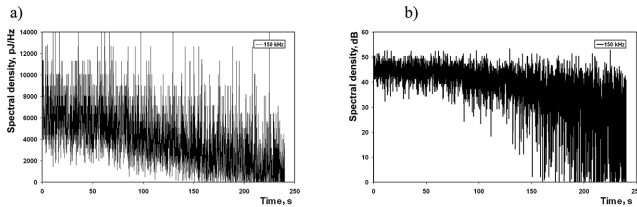

Fig. 11. Exemplary components of tested acoustic emission band from digital filtration for frequency of 150 kHz against time a) pJ/Hz , b) dB. Isothermal quenching at temperature 160°C

In order to make a spectrogram, the spectrum components were calculated as a function of time of consecutive 1647 samples using the method of Fourier analysis with windowing signal. Maximum values were for 150 kHz, Fig. 11. The relative values of spectrum components in relation to the spectrum components for selected value of frequency 400 kHz are shown in Fig. 12.
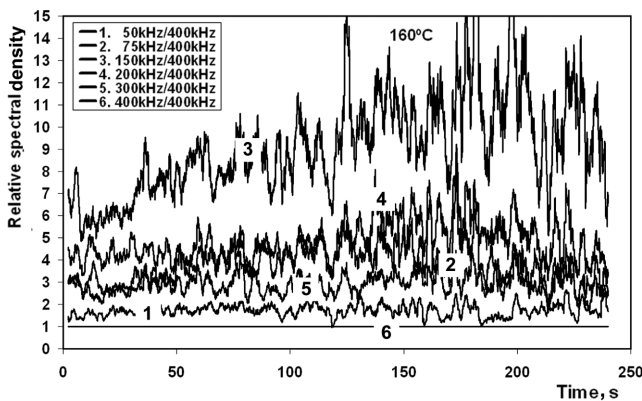

Fig. 12. Relative values of the components of the signal spectrum defined by digital filtering during isothermal quenching at 160°C, curves were drawn for arithmetic means from each 30 consecutive measurements (moving average)

Spectral characteristics for 80 samples of AE signals neighbouring on the signal maximum, for the analyses with the method for neural networks, shown in Fig. 13 consist of 80 coefficients. Each of them may take values within the range < 0...25 > decibels describing spectral interval power density in the bands of the frequency range width of 6.8 kHz. In each of the segments AE events are detected and an average energy of theses events is described. The frequency range from 6.8 kHz to 600 kHz is reproduced. High energy events in Fig. 13 curves Nr. 1, have maximum power density of spectrum located in the range of higher frequency (approx. 200 kHz), while the events of medium level, curves Nr. 2 – in the frequency range below 200 kHz. Power densities of AE spectra for low energy curves Nr. 3 have significantly lower values than power densities of medium and high power.
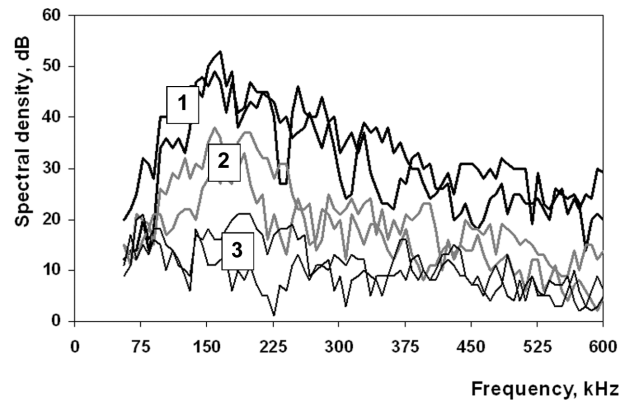

Fig. 13. Spectral density for 80 samples of acoustic emission signals neighbouring on the signal maximum as a function of frequency for selected segments of the events: 1) high energy, 2) medium energy, 3) low energy

Kinetic curves for lower bainite accelerated by small amounts of prior athermal martensite bainite and lover bainite were obtained by filtration of generated AE signal using neural network. Kinetic curves were obtained by filtering the generated signal of AE by using the neural network, Fig. 14.
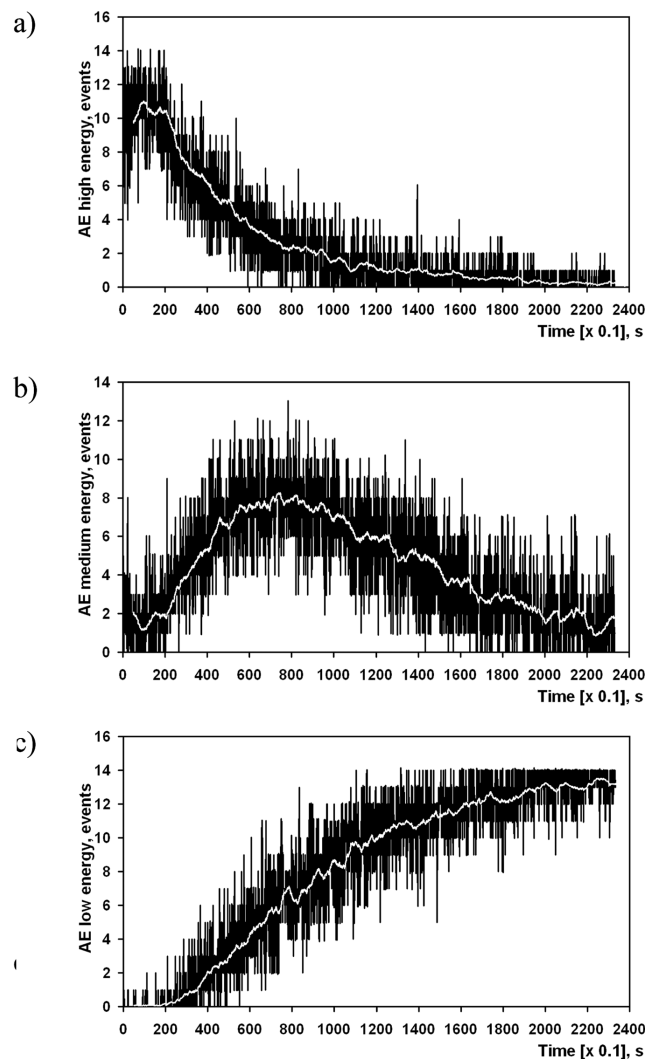

Fig. 14. Kinetic curves achieved by using the method of neural networks in time of first 4 minutes of austempering for a) small amounts of prior athermal martensite, b) lower bainite accelerated by small amounts of martensite, c) bainite formed at furthers

Phase transitions of bainitic type occur in three mutually overlapping stages. The first stage is a nucleation of small amounts of PAM during quenching Fig. 14 a) and its further increase at constant temperature of austempering. At second stage of transformation occurs acceleration of lower bainite transformation by small amounts of PAM Fig. 14 b). The third stage is connected with the enrichment of adhering austenite with carbon as a result of its diffusion outside previously generated martensite and bainite, which leads to its transformation into lower bainite Fig. 14 c). Both the kinetics of isothermal bainite transition and AE are also strictly connected with the release of carbides out of ferrite.

4. Discussion

The neural networks software identifies various-energy value AE events. It makes use of tabular recording of weight coefficients from signal spectral characteristics. This enabled the separation of AE events coming from various interfacing phase transformations, due to which it is possible to follow actual kinetics of phase transformation processes during austempering. The research shows that the method of AE is a sensitive tool to identify the mechanism of bainitic transformation and points to the interaction between martensitic and bainitic transformations. The occurrence of the AE phenomenon is connected with small amounts of PAM and bainite lath formation. Enriching austenite with carbon determines the bainitic transformation kinetics. The sources of AE recognised in metals are: dislocation movement resulting from plastic deformation, twin formation and displacive-type phase transformations [21-25]. Predominant source of AE during displacive transformations is the movement of dislocations. The shear mechanism and the movement of dislocations are strongly related. Strongly localized processes during a phase transformation lead to significant shear and dilatation, which make the main source of AE [26, 27]. Limited number of data available does not permit an unambiguous distinction between both types of AE sources. The AE technique is considered to be a good method to recognise the deforming character of the phase transformation.

The formation of a single lath or plate can involve many AE events, because the dislocation motion is related to the discontinuous interface movement. The AE signal generation by dislocation movements was a subject of research in a number of laboratories worldwide [14, 25, 28, 29]. AE is believed to originate from the propagation of high velocity (> 100 m/s) dislocation groups. About 40 dislocations, moving simultaneously, are required to give a detectable signal [30]. AE takes place when serious delays or dislocation-movement accelerations occur. N. Kiesewetter and P. Schiller [22] thought that acoustic waves were generated in active Frank-Read sources. A. Pawełek et al. [28, 29] showed that the synchronized annihilation of dislocation loop affected AE in a dominant way. Annihilation occurs when two opposite-orientation dislocations meet when the dislocation loops generated from Frank-Read sources are closing. Also twinning is an effective source of AE [31], which is a result of fast release of a large amount of elastic strain energy in a short time [32]. Only for twinned martensite one AE event was usually assumed to be related

to the formation of one martensite crystal [24]. Martensitic and bainitic transformations vary with the energy necessary to form one microarea of the plate, which results from another mechanism of transformation. Therefore, the characteristics of the signal emitted during the formation of the adequate plate will differ [33]. The spectral characteristic will be also different, which is connected with specific transformation dynamics. The bainite transformation involves less strain energy due to the shape change than during the growth of martensite [11]. The amount of plastic deformation during the growth of bainite is smaller. How the acoustic waves are generated during dislocation movement and how they are distorted by the equipment is not clearly understood.

The applied method allows the separation of emission signals corresponding to single plates. The analysed events differ in two parameters, i.e. in spectral characteristic and in energy. A minimum event, according to the used algorithm, includes three signal samples, i.e. 2.4 μs. The first program for neural networks divides the registered signal into segments with duration 7.35 ms. AE events are detected in each segment and the mean energy of the events is determined. To determine the spectral density function 80 standard samples neighbouring on the signal maximum were used, which corresponds with the time range of 67 μs. The spectral characteristics of the 80 signal samples were used in the neural network for learning procedure. As it results from the published research studies, the measured lengthening rate of the sub-unit is 75 microns per second [34]. It is sometimes assumed that the plate thickness is 0.2 μm and length 10 μm [35, 36]. The above shows that the minimum time growth of one of the sub-unit in bainite is about 3 ms. During this long time of one plate growth as many as 45 segments composed of 80 signal samples could be fitted. However, only one maximumamplitude segment of 80 samples was used to determine the spectral density function. The researchers who use the AE method generally accept the assumption that a single AE event is accompanied by the formation of a single martensite plate or a single slip caused by an increase in stress in the microarea [37].

For steel 100CrMnSi6-4 selected for the research, an area of cooled austenite transformation in range near M_S is very complex. It is generally connected with carbides in concentration bands called banding. The cementite in annealed steel makes, apart from temperature and time, an essential factor affecting the kinetics of the austenitizing process. In steel, after annealing in carbides $(Fe, Cr)_3C$, almost all carbon and a large amount of chromium and manganese are bonded. In areas where segregation and carbide banding occur, the concentrations of chromium or carbon may differ in particular places from mean values.

The addition of 1.5% of chromium in steel 100CrMnSi6-4 provides it with higher hardenability. After austenitizing, the solid solution is richer in carbon, chromium and manganese in bands with lower carbide content and the purpose of chromium is to provide hardenability, in particular. Chromium also moves the curve T'_0 towards lower carbon concentration, therefore, its content should be limited for bainitic transformations. The phenomenon of carbide banding and segregation contributes to significant diversity of matrix hardenability, which causes earlier formation of small amounts of PAM before the dilatometric curve bends clearly from the straight line. The formed

PAM amounts still do not show significant dilatometric effects, but they are very important as regards their structure, being precursors of the accelerated bainitic transformation. The occurrence range for acceleration of lower bainite transformation by small amounts of PAM differs depending on carbon content in steel [3]. T.Z. Wozniak proved in his earlier research [5, 7] that acoustic effects during *midrib* formation are many times higher than during the formation of further bainite Shares. In recent years, D. H. Kim et al. [38] have proved that there is a significant difference between isothermal transformation above temperature M_S, i.e. in the temperature range where bainite is formed, and isothermal transformation below M_S. It has been concluded earlier that isothermal transformation below temperature M_S is not a typical low-temperature continuation of bainitic disintegration [39].

The phenomenon of carbon diffusion between martensite and residual austenite tends to be avoided in steel after customary quenching for the sake of too low temperature. Martensite carbon-saturation is usually reduced by a mechanism of carbide educing during tempering. The mechanism of bainitic transformation shows that when the growth of particular bainite laths is completed, carbon is redistributed to untransformed austenite, or carbides are educed [1, 19, 40]. Bainitic transformation stops when austenite is enriched with carbon to the value defined by curve T_0' and driving force by shear mechanism becomes reduced to zero. Carbon-rich austenite is more shear-resistant, which increases the driving force required to bainite formation. The process of carbide ε educing reduces carbon concentration in austenite below curve T_0', which initiates further bainitic transformation. Applying neural networks, the kinetics of prolonged bainitic transformation was determined. The research results, with use of neural networks, show that at quenching temperature 160°C occurs an equilibrium state between the enriching of untransformed austenite with carbon and the processes of carbide ε educing. This results in further bainitic transformation and prolonged AE.

5. Conclusions

A favourable effect of martensitic transformation on bainitic transformation acceleration was already observed in bearing steels. Heat treatment operations consisted in cooling below M_S with later increase in temperature to the bainitic range. The present study suggests original isothermal austempering with bainitic transformation during which small amounts of prior athermal martensite (PAM) are initially formed as a result of chemical heterogeneity. The processes that take place during the formation of bainite on small amounts of PAM generate exceptionally high-energy signals.

1. Bainitic and martensitic microstructure with carbide particles of complex dispersion was obtained. The phase transformation kinetics was researched with use of the acoustic emission (AE) method and neural networks.
2. In a very large number of AE event population occur alternately three types of events with high, medium and low energies and for that reason their separation required a special procedure. The method consisted in separating the three types of events, considering not only the energy level but also different spectral characteristics.
3. The software that identifies different-energy AE events values and uses the possibility of tabular retention of weight coefficients of neural networks allows the separation of AE events from various physical phenomena and the monitoring of the processes that occur during phase transformations.
4. Phase transformations in steel 100CrMnSi6-4 during isothermal austempering vary due to banding. Bright martensitic bands occur next to the dark ones with martensitic-bainitic matrix (with a larger content of carbides).
5. The results obtained by AE method show that bainitic transformation occurs by shear mechanism and austenite disintegration at 160°C is of both martensitic-bainitic and bainitic character.
6. The dominating area where over-cooled austenite transforms into lower bainite accelerated by small amounts of PAM in steel 100CrMnSi6-4 occurs in the range near M_S. Spectral range of signals is constant and is from 100 to 300 kHz. Maximal spectral density occurs at frequency from 180 to 200 kHz.
7. The AE method may be successfully applied for kinetics of complex phase transformations occurring in steel 100CrMnSi6-4 and in other steels under the processes of quenching. The assessment on the initial phase of martensite formation with use of typical dilatometric methods is based on macroscopic effects of geometric changes while the suggested AE method is based on changes in microscopy scale.

REFERENCES

[1] J.G. Speer, D.K. Matlock, B.C. De Cooman, J.G. Schroth, Acta Materialia **51**, 2611 (2003).
[2] H. El Kadiri, L. Wang, M.F. Horstemeyer, R.S. Yassar, J.T. Berry, S. Felicelli, P.T. Wang, Materials Science and Engineering A **494**, 10 (2008).
[3] M. Oka, H. Okamoto, Metallurgical and Materials Transactions A **19A**, 447 (1988).
[4] S.M.C. Van Bohemen, M.J. Santofimiaa, J. Sietsma, Scripta Materialia **58**, 488 (2008).
[5] T.Z. Woźniak, Z. Ranachowski, Archives of Acoustics **31**, 3 (2006).

[6] T.Z. Woźniak, Materials Science and Engineering A **408**, 309 (2005), DOI: 10.1016/j.msea.2005.08.148.

[7] T.Z. Woźniak, Materials Characterization **59**(6), 708 (2008), DOI: 10.1016/j.matchar.2007.06.004.

[8] D. Kim, J.G. Speer, B.C. De Cooman, Metallurgical and Materials Transactions A **42**(6), 1575 (2010).

[9] T. Chandra, N. Wanderka, W. Reimers, M. Ionescu, Materials Science Forum **638-642**, 3307 (2010).

[10] J. Sun, H. Lu, M. Kang, Metallurgical and Materials Transactions A **23**, 2483 (1992).

[11] H.K.D.H. Bhadeshia, Bainite in Steels, 2-nd ed. The Institute of Materials, London 2001.

[12] H.K.D.H. Bhadeshia, C.H. Young, Materials Science and Technology **10**, 209 (1994).

[13] C. Li, J.L. Wang, Journal of Materials Science **28**, 2112 (1993).

[14] S.M.C. Van Bohemen, An acoustic emission study of martensitic and bainitic transformations in carbon steel, University Press Delft 2004.

[15] C.K. Shui, W.T. Reynolds Jr., G.J. Shiflet, H.I. Aaronson, Metallography **21**, 91 (1988).

[16] C. Garcíade Andrés, F.G. Caballero, C. Capdevila, L.F. Álvarez, Materials Characterization **48**, 101 (2002).

[17] S.M.C. Van Bohemen, J. Sietsma, Metall. Mater. Trans. A **40**, 1059 (2009).

[18] T.Z. Woźniak, J. Jeleńkowski, K. Rożniatowski, Z. Ranachowski, Materials Science Forum **726**, 55 (2012), DOI: 10.4028/www.scientific.net/MSF.726.55.

[19] T.Z. Woźniak, K. Rożniatowski, Z. Ranachowski, Kovove Materialy- Metallic Materials **49**, 319 (2011). DOI: 10.4149/km_2011_5_319.

[20] T.Z. Woźniak, K. Rożniatowski, Z. Ranachowski, Metals and Materials International **17**, 365 (2011), DOI: 10.1007/s12540-011-0611-4.

[21] P.C. Clapp, J. Phys. IV 5, C8-11 (1995).

[22] N. Kiesewetter, P. Schiller, Phys. Stat. Sol. A **38**, 569 (1976).

[23] A. Lambert, X. Garat, T. Sturel, A.F. Gourgues, A. Gingell, Scripta Mater. **43**, 161 (2000).

[24] L.I. Manosa, A. Planes, D. Rouby, J.L. Macqueron, Acta Metallurgica et Materialia **38**, 1635 (1990).

[25] H.N.G. Wadley, C.B. Scruby, J.H. Speake, Int. Metals Rev. **25**, 41 (1980).

[26] R.W.K. Honeycombe, H.K.D.H. Bhadeshia, Steels – Microstructure and Properties (2nd ed.), Edward Arnold, London 1995.

[27] D.A. Porter, K.E. Easterling, Phase Transformations in Metals and Alloys., 2nd ed., Chapman and Hall, London 1992.

[28] A. Pawełek, Journal of Applied Physics **63**, 5320 (1988).

[29] A. Pawełek, Journal of Applied Physics **62**, 2549 (1987).

[30] C. Scruby, H.J. Wadley, Journal of Mater. Sci. **28**, 2501 (1993).

[31] T. Bidlingmaier, A. Wanner, G. Dehm, H. Clemens, Z. Metallkd. **90**, 581 (1999).

[32] V.S. Boiko, Phys. Stat. Sol.(b) **55**, 477 (1973).

[33] S.M.C. Van Bohemen, M.J.M. Hermans, G. Den Ouden, Materials Science and Technology **18**, 1524 (2002).

[34] H.K.D.H. Bhadeshia, Proceedings of an International Conference on Phase Transformations in Ferrous Alloys, eds A. Marder and J. Goldstein, Philadelphia, A.I.M.E, 335-340 (1984).

[35] H.K.D.H. Bhadeshia, J. Phys. Paris **C43** (Colloq. C4), 443 (1982).

[36] G.I. Rees, H.K.D.H. Bhadeshia, Mater. Sci. Technol. **8**, 994 (1992).

[37] R.M. Fisher, J.S. Lally, Canadian Journal of Physics **45**, 1147 (1967).

[38] D.H. Kim, J.G. Speer, H.S. Kim, B.C. De Cooman, Metall. Mater. Trans. A **40**, 2048 (2009).

[39] H.K.D.H. Bhadeshia, J.W. Christian, Metallurgical and Materials Transactions A **21**, 767 (1990).

[40] A.J. Clarke, J.G. Speer, M.K. Miller, R.E. Hackenberg, D.V. Edmonds, D.K. Matlock, F.C. Rizzo, K.D. Clarke, E. De Moor, Acta Materialia **56**, 16 (2008).